



Contents lists available at ScienceDirect

Journal of Computational and Applied Mathematics

journal homepage: www.elsevier.com/locate/cam

Existence and stability of stationary waves of a population model with strong Allee effect

Majid Bani-Yaghoub^{a,*}, Guangming Yao^b, Hristo Voulouf^a^a Department of Mathematics and Statistics, University of Missouri-Kansas City, Kansas City, MO 64110-2499, USA^b Department of Mathematics, Clarkson University, Potsdam, NY, 13699-5815, USA

ARTICLE INFO

Article history:

Received 31 July 2015

Received in revised form 23 November 2015

MSC:
37N25
35R10

Keywords:

Allee effect
Delay
Reaction–diffusion
Nonlocality
Stationary wave

ABSTRACT

We investigate the existence and stability of stationary waves of a nonlocal reaction–diffusion population model with delay, nonlocality and strong Allee effect. By reducing the model, the conditions for existence of stationary wavefront, wave pulse and inverted wave pulse are established. Then we show that the stationary waves of the reduced model are also the stationary waves of the general model. The global stability of the stationary waves is illustrated by numerically solving the general model for different sets of parameter values.

© 2015 Elsevier B.V. All rights reserved.

1. Introduction

The wave solutions of Reaction–Diffusion (RD) models have been center of attention for decades [1–4]. In addition to vast applications of traveling waves in population biology [5,3,6], various forms of waves have been observed in chemical reactions [1,7,8], nonlinear optics [9], water waves [10–12], gas dynamics [13] and solid mechanics [14–17]. In order to define the wave solutions of RD models, consider the following scalar RD equation

$$\frac{du(x, t)}{dt} = D \frac{\partial^2 u(x, t)}{\partial x^2} + f(u(x, t)), \quad (1)$$

where $u(x, t) \in \mathbb{R}$ is for instance, the population density of a single species at time t and location $x \in \mathbb{R}$, $f(u)$ is the proliferation rate, and D is the diffusion rate of the single species. A traveling wave solution $u(x, t)$ of Eq. (1) is a solution of the form

$$u(x, t) = U(x + ct) = U(z), \quad z = x + ct, \quad \text{with } x \in \mathbb{R} \text{ and } t > 0, \quad (2)$$

where the constant c is the speed of propagation and the dependent variable z is the wave variable. Then $U(z)$ is a traveling wave moving at constant speed c without changing its shape or amplitude. To be physically realistic, $U(z)$ must be bounded

* Corresponding author.

E-mail address: baniyaghoubm@umkc.edu (M. Bani-Yaghoub).<http://dx.doi.org/10.1016/j.cam.2015.11.021>

0377-0427/© 2015 Elsevier B.V. All rights reserved.

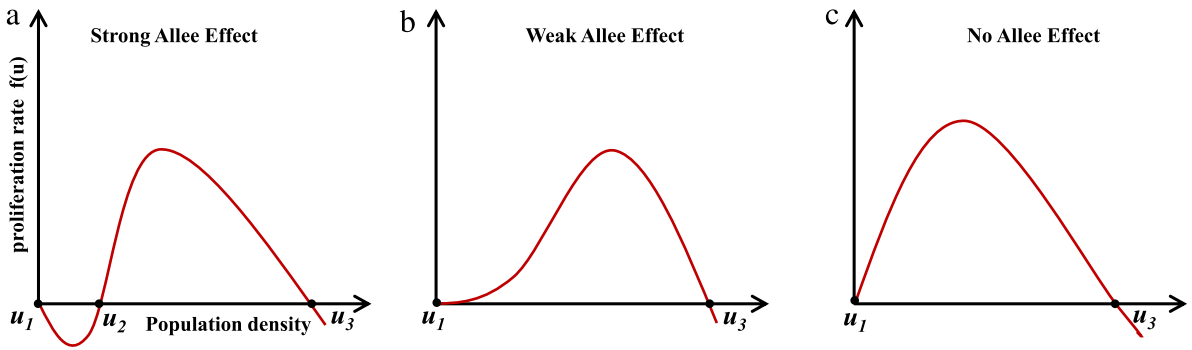


Fig. 1. A schematic representation of density dependence. (a) With strong Allee effect there is a threshold value u_2 at low population densities and $f(u)$ is concave up at the origin. (b) With weak Allee effect there is no threshold value, yet $f(u)$ remains concave up at the origin. (c) There is no Allee effect when $f(u)$ is concave down at the origin.

and non-negative for all $z \in \mathbb{R}$. When $c = 0$, the wave is stationary (i.e., it does not travel in any direction of the spatial domain).

By substituting $U(z)$ into Eq. (1) and using the chain rule, the wave equation

$$D \frac{d^2U(z)}{dz^2} - c \frac{dU(z)}{dz} + f(U(z)) = 0 \tag{3}$$

is deduced.

Let $c = 0$ and let zero and one be the equilibria of Eq. (3). Then a solution of Eq. (3) that satisfies boundary conditions $U(-\infty) = 0$ and $U(\infty) = 1$ is a stationary wavefront of Eq. (1). Similarly, the stationary wave pulse of the RD equation (1) satisfies the wave equation (3) and boundary conditions $U(\pm\infty) = 0$. The wave pulse is inverted when the boundary condition is changed to $U(\pm\infty) = 1$. The stationary front and pulse solutions of the RD equation (1) are respectively characterized by the homoclinic and heteroclinic orbits [18,19] of Eq. (3) in the corresponding phase-planes.

The present work investigates the existence and stability of stationary pulse and wavefronts of an RD population model with delay, nonlocality and strong Allee effect [20,21]. A population exhibits Allee effect when its proliferation rate $f(u)$ is negative or close to zero at low population densities (i.e., $f(u)$ is concave up at the origin). For larger population densities, $f(u)$ increases until it reaches a local maximum. The difference between the strong and weak Allee effect is shown in Fig. 1, where the former has a critical population density u_2 while the latter does not. In the absence of diffusion, a population with strong Allee effect goes extinct when the density falls below the threshold value u_2 . In the present work we show that the threshold value u_2 does not necessarily determine the fate of single species when the diffusion is present. In other words, the population dispersal can be used as a survival mechanism for single species with some densities below u_2 . Without loss of generality, let $u_1 = 0$, $u_2 = T$ and $u_3 = 1$. Then $f(u)$ with strong Allee effect is mathematically characterized by

- (H₁) $f(0) = f(T) = f(1) = 0$
- (H₂) $f(u) < 0, 0 < u < T$
- (H₃) $f(u) > 0, T < u < 1$
- (H₄) $f'(0) < 0, f'(T) > 0, f'(1) < 0$.

Let $w(x, t)$ be the population density of the mature population at time t and position x . Then nonlocal delayed RD model is given by

$$\frac{\partial w(x, t)}{\partial t} = D_m \frac{\partial^2 w(x, t)}{\partial x^2} - d_m w(x, t) + \epsilon \int_{-\infty}^{\infty} b(w(y, t - \tau)) f_{\alpha}(x - y) dy, \quad \text{for } t > \tau, \tag{4}$$

where D_m and d_m are respectively constant diffusion and death rates of the mature population, $\tau > 0$ is the maturation time delay, $b(w)$ is the birth function and

$$f_{\alpha}(x) = \frac{1}{\sqrt{4\pi\alpha}} \exp\left(\frac{-x^2}{4\alpha}\right), \tag{5}$$

is the heat kernel. Let $d_I(\theta)$ be the death rate of individuals at age θ . Then the constant ϵ is given by

$$\epsilon = \exp\left\{-\int_0^{\tau} d_I(\theta) d\theta\right\}, \tag{6}$$

which represents the overall impact of the immature population death on the mature population growth rate. The integral term in the model (4) is a weighted spatial average corresponding to all births occurred in the spatial domain at a previous time $t - \tau$. Using the Britton's approach [22,23] and the Smith–Thieme approach [24] model (4) was developed by So et al. [6].

The impact of the density dependent birth function $b(w)$ and maturation time delay τ on single species population dynamics has been studied in detail [25,26]. Model (4) has also been extended to RD models with respect to two-dimensional spatial domains [25–27], where the existence of traveling wave solutions has been investigated [26,6].

The diffusion rate of the immature population is given by $D_I = \alpha/\tau$. Hence, the immature population is immobile when $\alpha = 0$ and the general model (4) is reduced to

$$\frac{\partial w(x, t)}{\partial t} = D_m \frac{\partial^2 w}{\partial x^2} - d_m w(x, t) + \epsilon b(w(x, t - \tau)), \tag{7}$$

which has been extensively studied [28–30].

Let $w(x, t) = \phi(x + ct) = \phi(z)$ be a wave solution of the general model (4). Let $Y = y - x$ and $z = x + ct$. Define the linear transformation $T(t, x) = x + ct$ and let $w(x, t) = \phi(z)$ be the wave solution. Then substituting $\phi(z)$ into (4), using the transformation $T(t - \tau, y) = z - c\tau + Y$, and replacing Y with y , the wave equation corresponding to (4) is given by

$$D_m \phi''(z) - c \phi'(z) - d_m \phi(z) + \epsilon \int_{-\infty}^{\infty} b(\phi(z - c\tau + y)) f_\alpha(y) dy = 0. \tag{8}$$

The minimal speed of spread and the existence of traveling wavefronts of the model (4) have already been investigated in several studies [5,31,6]. Using specific birth functions, the behavior of wave solutions has been studied in [5,32,26]. The traveling wave solution of model (4) can be approximated using a boundary layer method combined with an asymptotic expansion method [33]. Despite the above-mentioned studies, there has been less effort investigating the existence and stability of the stationary waves of the model (4). The present work aims to fill this gap by establishing the conditions for existence of stationary waves (Section 2) and numerically examining the stability of the stationary wave solutions (Section 3). Furthermore, a discussion of the main outcomes and the biological implications of the results is provided in Section 4.

2. Existence of stationary waves

Let $c = 0$ and $U(z) = \phi(x)$. Then wave equation (3) is reduced to the Hamiltonian system

$$\begin{cases} \frac{d\phi(x)}{dx} = \varphi(x) \\ \frac{d\varphi(x)}{dx} = -\frac{1}{D} f(\phi(x)), \end{cases} \tag{9}$$

with the Hamiltonian function

$$\mathcal{H}(\phi, \varphi) = \frac{\varphi^2}{2} + \frac{1}{D} \int_0^\phi f(s) ds. \tag{10}$$

Define

$$F(\phi) = \frac{1}{D} \int_0^\phi f(s) ds. \tag{11}$$

The following theorem establishes the conditions for existence of homoclinic and heteroclinic orbits of the system (9).

Theorem 1. *Let $f(\phi)$ be continuous and satisfy conditions (H_1) – (H_4) . Then system (9) admits a*

- (i) *right-homoclinic orbit, when $F(1) > 0$*
- (ii) *left-homoclinic orbit, when $F(1) < 0$*
- (iii) *heteroclinic orbit, when $F(1) = 0$.*

Proof. Part (i)

Each level curve of the system (9) is given by $\mathcal{H}(\phi, \varphi) = k$, where k is a constant. Noting that $\mathcal{H}(0, 0) = 0$ for a right-homoclinic orbit, we must have $k = 0$. Using (10) the level curve passing through the origin must satisfy $\varphi^2 = -2F(\phi)$. By conditions (H_1) and (H_2) we get that $F(0) = 0$ and $F(\phi) < 0$ for $\phi \in (0, T]$. Since $F(1) > 0$, there must be a point $\phi^* \in (T, 1)$ such that $F(\phi^*) = 0$. By the continuity of $F(\phi)$ we conclude that there exists a homoclinic orbit connecting the origin to itself.

Part (ii)

A left-homoclinic orbit connects $(\phi, \varphi) = (1, 0)$ to itself. Consider the slightly modified Hamiltonian function

$$\hat{\mathcal{H}}(\phi, \varphi) = \frac{\varphi^2}{2} - \frac{1}{D} \int_\phi^1 f(s) ds. \tag{12}$$

Similar to part (i), for the level curve passing through $(1, 0)$, we must have $k = 0$ and therefore $\varphi^2 = \frac{2}{D} \int_{\phi}^1 f(s)ds$. By conditions (H_1) and (H_4) the last integral has a maximum at $\phi = T$ and declines in the interval $\phi \in (T, 1)$. Noting that $F(1) < 0$, there must be a point $\phi^* \in (0, T)$ such that $\varphi = 0$.

Part (iii)

A heteroclinic orbit connects the origin to $(\phi, \varphi) = (1, 0)$. Since $F(1) = 0$ we must have $\int_T^1 f(s)ds = -\int_0^T f(s)ds$. Using the Hamiltonian function (10) we get that $\phi^* = 1$. □

A non-constant stationary solution $w(x, t) = \phi(x)$ of the reduced model (7) must satisfy

$$D_m \phi''(x) - d_m \phi(x) + \epsilon b(\phi(x)) = 0. \tag{13}$$

Then we have the following corollary.

Corollary 1. Let $f(\phi) = \epsilon b(\phi) - d_m \phi$ and satisfy conditions (H_1) – (H_4) . Then the reduced model (7) admits a stationary

- (i) wave pulse, when $F(1) > 0$
- (ii) inverted wave pulse, when $F(1) < 0$
- (iii) wavefront, when $F(1) = 0$.

Proof. This is a direct implication of Theorem 1. □

We now turn our attention to the specific birth function given by

$$b(\phi) = p\phi^2 e^{-a\phi}, \tag{14}$$

which has been frequently used in different studies [32,31,26,6]. The single species population can exhibit strong Allee effect, when the birth function (14) is employed. The following lemma provides details of the possible equilibria of models (4) and (7) with the birth function (14).

Lemma 1. Let $b(\phi) = p\phi^2 e^{-a\phi}$. Let $\epsilon p/d_m = e^r a/r$ for $r > 0$ and $r \neq 1$. Then the reduced and general models (7) and (4) both admit constant equilibria $\phi_1 = 0, 0 < \phi_2 < \phi_3$ and $\phi_3 = r/a$.

Proof. A constant equilibrium ϕ_i of the reduced model (7) is also that of the general model (4) and it satisfies $\epsilon b(\phi_i) - d_m \phi_i = 0$. When $b(\phi) = p\phi^2 e^{-a\phi}$, $\phi_1 = 0$ is an equilibrium. Provided that $r > 0$ and $r \neq 1$, there are two positive equilibria

$$\phi_2 = -W_0(-ad_m/\epsilon p)/a \quad \text{and} \quad \phi_3 = -W_{-1}(-ad_m/\epsilon p)/a,$$

where $W_0(x)$ and $W_{-1}(x)$ represent the real-valued principal and the lower branches of Lambert $W(x)$ function, for $x \in (-e^{-1}, 0)$. Using $\epsilon p/d_m = e^r a/r$ we get that $\phi_3 = r/a$ and $0 < \phi_2 < \phi_3$. □

The following corollary establishes the conditions for existence of stationary waves of the reduced model (7), when the birth function (14) is employed.

Corollary 2. Let $b(\phi) = p\phi^2 e^{-a\phi}$. Let $h(r) = -2e^r/r + r^2/2 + r + 2 + 2/r, r \neq 1$ and $\epsilon p/d_m = e^r a/r$. Then the reduced model (7) admits a stationary

- (i) wave pulse, when $h(r) < 0$
- (ii) inverted wave pulse, when $h(r) > 0$
- (iii) wavefront, when $h(r) = 0$.

Proof. Noting that $f(\phi) = \epsilon b(\phi) - d_m \phi$ from Eq. (14) we have

$$\int f(\phi)d\phi = -\epsilon p \left(\frac{a^2 \phi^2 + 2a\phi + 2}{a^3} e^{-a\phi} \right) - \frac{d_m}{2} \phi^2. \tag{15}$$

Part (i) Using Theorem 1 we only need to show that $F(1) > 0$ or equivalently

$$\int_{\phi_2}^{\phi_3} f(\phi)d\phi > -\int_0^{\phi_2} f(\phi)d\phi. \tag{16}$$

Using Eq. (15) and noting that the equilibria $\phi_i, i = 1, 2, 3$ satisfy $d_m \phi = \epsilon p \phi^2 e^{-a\phi}$ we get that the inequality (16) is the same as

$$d_m \left(\frac{\phi_3^2}{2} + \frac{\phi_3}{a} + \frac{2}{a^2} + \frac{2}{a^3 \phi_3} \right) < \frac{2\epsilon p}{a^3}. \tag{17}$$

By Lemma 1 $\phi_3 = r/a$. Also $\epsilon p/d_m = e^r a/r$. Hence the last inequality is the same as $h(r) < 0$. Proofs of parts (ii) and (iii) are similar to the proof of part (i). □

Remark 1. Note that the root of $h(r)$ is $r = 1.451$. Hence, under the assumptions of [Corollary 2](#) the reduced model (7) admits a stationary wavefront when $r = 1.451$. Similarly, the existence of inverted wave pulse and wave pulse are implied by $r < 1.451$ and $r > 1.451$, respectively.

The following theorem indicates that the stationary pulse and front solutions of the reduced model (7) are also those of the general model (4). The proof is based on the generalized mean value theorem and the properties of the heat kernel $f_\alpha(x)$.

Remark 2. Let $f(x)$ and $g(x)$ be continuous functions. Let $f(x) \geq 0$ for all $x \in \mathbb{R}$ and $a, b > 0$. Then by the mean value theorem for integrals (e.g., [34, page 409]), there exists a constant $k > 0$ such that

$$\int_{-a}^b g(t)f(t)dt = g(k) \int_{-a}^b f(t)dt. \tag{18}$$

Theorem 2. Let $\phi(x)$ be a stationary front, pulse or inverted pulse of the reduced model (7). Then $\phi(x)$ is also a stationary front, pulse or inverted pulse of the general model (4), respectively.

Proof. Let $\phi(x)$ be the stationary front of the reduced model (7) that connects the equilibria ϕ_+ and ϕ_- at the two ends. Then $\phi(x)$ satisfies

$$D_m\phi''(x) - d_m\phi(x) + \epsilon b(\phi(x)) = 0. \tag{19}$$

We need to show that $\phi(x)$ also satisfies the wave equation of the general model (4), which is

$$D_m\phi''(x) - d_m\phi(x) + \epsilon \int_{-\infty}^{\infty} b(\phi(y))f_\alpha(x - y)dy = 0. \tag{20}$$

Let $z = y - x - v$, where v is a constant which is determined later. Noting that $f_\alpha(x)$ defined in (5) has the property $f_\alpha(x - y) = f_\alpha(y - x)$, Eq. (20) is rewritten

$$D_m\phi''(z) - d_m\phi(z) + \epsilon \int_{-\infty}^{\infty} b(\phi(z + x + v))f_\alpha(z + v)dz = 0. \tag{21}$$

Hence, we need to show that for each $x \in \mathbb{R}$,

$$\int_{-\infty}^{\infty} b(\phi(z + x + v))f_\alpha(z + v)dz = b(\phi(x)). \tag{22}$$

Let a and b be positive constants. Noting that $b(\phi(z + x))$ and $f_\alpha(z)$ are continuous and $f_\alpha(z) > 0$ for all $z \in \mathbb{R}$, by [Remark 2](#), for each $x \in \mathbb{R}$ there exists a constant $k \in (-a, b)$ such that

$$\int_{-a}^b b(\phi(z + x + v))f_\alpha(z + v)dz = b(\phi(k + x + v)) \int_{-a}^b f_\alpha(z + v)dz. \tag{23}$$

The value of k depends on a and b . However, the only extrema of $f_\alpha(z)$ is the global maximum at $z = 0$ and $\lim_{z \rightarrow -\infty} f_\alpha(z) = 0$ and $\lim_{z \rightarrow \infty} f_\alpha(z) = 0$, as $z \rightarrow \pm\infty$.

Also the integrals in (23) are convergent and $\int_{-\infty}^{\infty} f_\alpha(z + v)dz = 1$. Hence by letting $a, b \rightarrow \infty$, k converges to a single value k^* , where $v = k^*$ implies Eq. (22). The proof for the stationary pulse or inverted pulse is similar. \square

3. Stability of stationary waves

Stability of stationary wave solutions was numerically investigated by solving the initial value problem corresponding to the general model (4) and the wave equation (13). In particular, we employed a finite difference scheme in Matlab 2014a to solve and compare the PDE solutions of (4) with the stationary wave solutions of (13) for different sets of parameter values. When a stationary wave solution exists, the choice of the initial history function can play a critical role in convergence of the PDE solution to the wave solution or to the constant equilibria. By considering the birth function (14), there are three constant equilibria $\phi_1 = 0$, $\phi_2 = -W_0(-ad_m/\epsilon p)/a$ and $\phi_3 = -W_{-1}(-ad_m/\epsilon p)/a$, provided $\epsilon p/d_m > ae$. Noting that ϕ_1 and ϕ_3 are stable and ϕ_2 is unstable, we need to choose a history function $w_0(x, t)$ with values below and above ϕ_2 . Otherwise the PDE solution converges to ϕ_1 regardless of the delay value τ or it converges to ϕ_3 for small values of τ . We considered the initial history function

$$w_0(x, t) = \phi_2 - y_0 + \beta/(1 + \exp(-\delta(x - 210))) \quad \text{for } t \in [-\tau, 0] \tag{24}$$

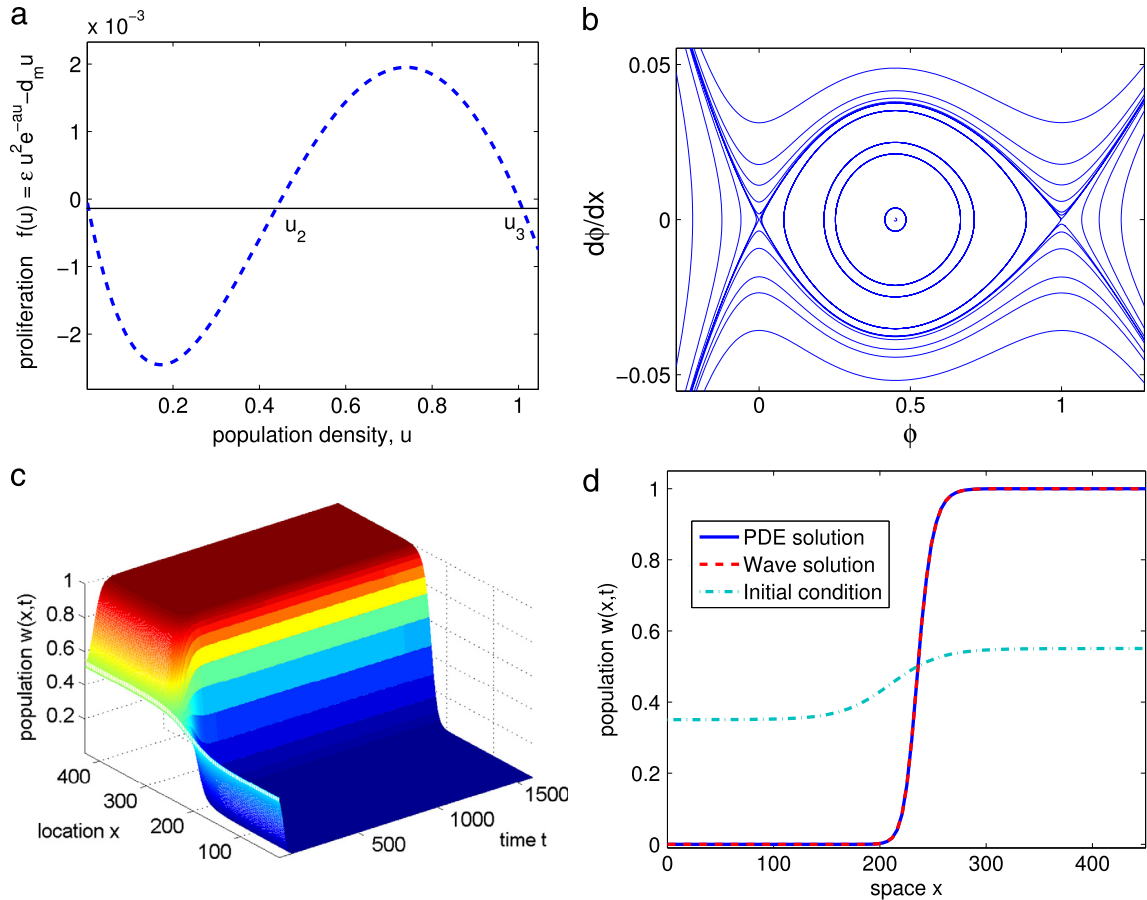


Fig. 2. The solution of the general model (4) may converge to the stationary wavefront. (a) Graph of the proliferation function $f(u) = \epsilon b(u) - d_m u$, where $b(u)$ and $F(\phi)$ are defined in (14) and (11), respectively. Note that $F(1) = 0$, i.e., the areas surrounded by $f(u)$ and u -axis are equal. (b) Phase-plane of the system (9) representing the heteroclinic orbit. (c and d) Convergence of the solution $w(x, t)$ of the general model (4) to the stationary wavefront $\phi(x)$ of the wave equation (13). See the supplementary file “confront.gif” for the related animation (see Appendix A). The specific parameter values are given in Table 1.

Table 1

Summary of the parameter values used for the numerical simulations illustrated in Figs. 2–4. We used birth function (14) with strong Allee effect for the simulations.

Symbol	Description of parameters and variables	Specific parameter values		
		Fig. 2	Fig. 3	Fig. 4
d_m	Death rate of mature population	0.1	0.1	0.1
p	Mating ratio	4.27	4.95	3.67
ϵ	Total death rate of immature population	0.1	0.1	0.1
D_m	Diffusion rate of mature population	3.0	3.0	3.0
D_I	Diffusion rate of immature population	1.0	1.0	1.0
a	Overcrowding parameter	1.45	1.60	1.30
τ	Maturation time delay	1.0	1.0	1.0
w_2	The equilibrium between 0 and	0.45	0.36	0.58
y_0	Parameter of the history function	0.1	0.1	0.07
β	Parameter of the history function	0.2	0.2	0.1
δ	Parameter of the history function	0.043	0.001	0.008

Notes. The initial history function for Fig. 2 is given by (24). Also the initial history function for Figs. 3 and 4 is given by (25). Similar results were obtained using different sets of parameter values.

and

$$w_0(x, t) = \phi_2 - y_0 + \beta \exp(-\delta(x - 200)) \quad \text{for } t \in [-\tau, 0] \tag{25}$$

to investigate the convergence to the stationary wavefront and wave pulses, respectively. Table 1 is a summary of the specific parameter values including the constants β , δ and y_0 .

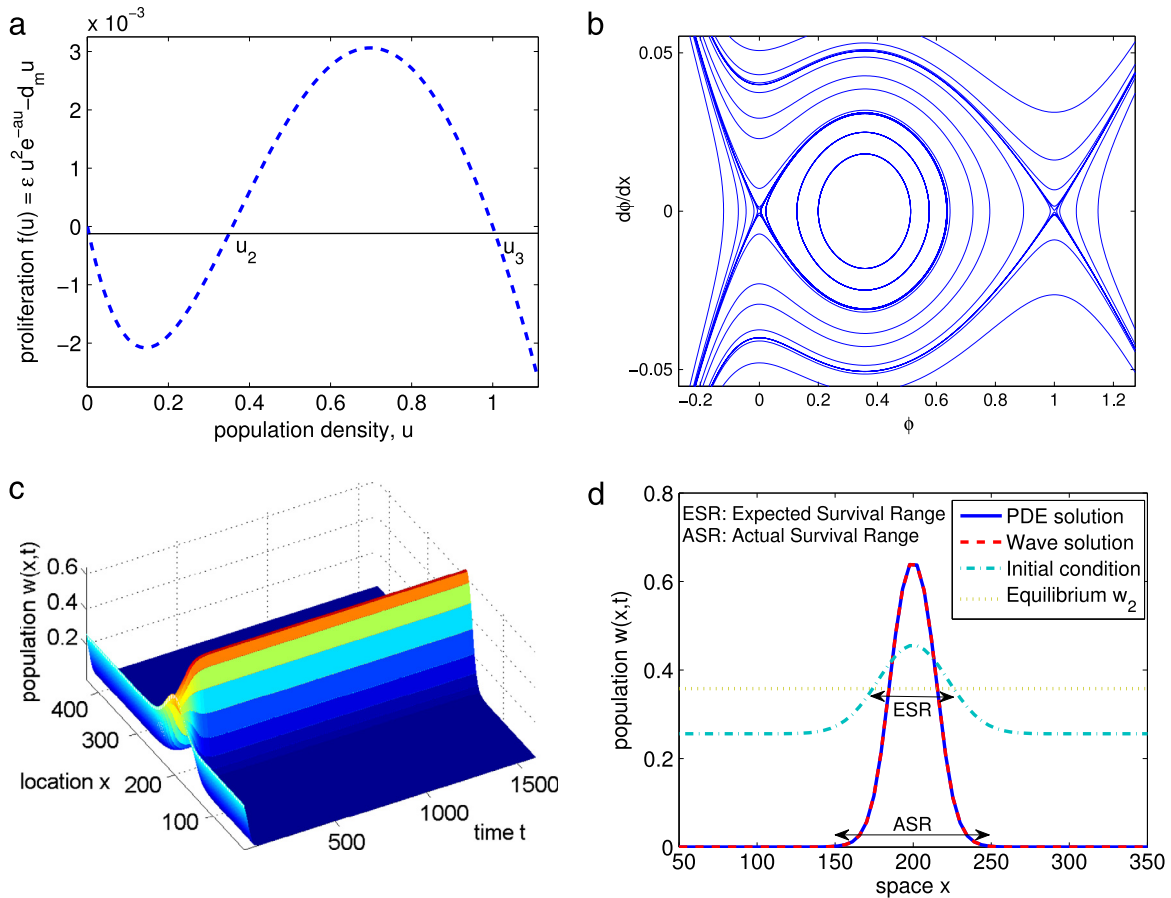


Fig. 3. The solution of the general model (4) may converge to the stationary wave pulse. (a) Graph of the proliferation function $f(u) = \epsilon b(u) - d_m u$, where $b(u)$ is defined in (14). Note that $F(1) > 0$, i.e., the area above $f(u)$, $u \in [0, u_2]$ is less than the area under $f(u)$, $u \in [u_2, u_3]$. (b) Phase-plane of system (9) representing a right-homoclinic orbit. (c and d) Convergence of the solution $w(x, t)$ of model (4) to the stationary wave pulse $\phi(x)$ of wave equation (13). See the supplementary file “conpulse.gif” for the related animation (see Appendix A). The expected and actual survival ranges correspond to the absence and presence of diffusion, respectively. It can be seen that the survival range is increased when the diffusion is present. The specific parameter values are given in Table 1.

Fig. 2 shows that the solution of the general model (4) may converge to the stationary wavefront satisfying both Eqs. (8) and (13). Specifically, as shown in panel (a), the existence of the heteroclinic orbit is only possible when $F(1) = 0$ (see Corollary 1 part (iii)). Panel (b) illustrates the phase-plane of the system (9) representing the heteroclinic orbit, which is equivalent to a stationary wavefront. The convergence of the PDE solution to the stationary wavefront is shown in panels (c) and (d). The convergence is animated in “confront.gif” which is available in the supplementary documents (see Appendix A). The specific parameter values are given in Table 1. Further numerical simulations are presented in Figs. 3 and 4, where the convergence to the stationary wave pulse and inverted wave pulse are shown, respectively. The animation related to the PDE solution converging to wave pulse is available in the supplementary documents (see file “conpulse.gif”, Appendix A). Also the file “coninvertpulse.gif” is the animation for convergence of the PDE solution to the inverted pulse wave. We also explored the convergence to the stationary wave solutions for different sets of the parameter values. When the maturation time delay τ is increased the stability of ϕ_3 is lost for the cases $F(1) \geq 0$ (see Theorem 3(iii) of [32]) and therefore convergence to the stationary wavefront and wave pulse does not occur. Nevertheless, the stability of ϕ_3 is delay independent for the case $F(1) < 0$ ([32, Theorem 3(i)]) and the PDE solution may converge to the inverted wave pulse (see Fig. 4) regardless of τ value.

In addition to convergence to the stationary pulse, panel (d) of Fig. 3 shows that the threshold property of the middle equilibrium $w_2 = T$ does not hold valid when the diffusion is present. In particular, the Expected Survival Range (ESR) indicates the regions with the initial population densities above the threshold T and single species with initial densities below T is expected to go extinct. Whereas the Actual Survival Range (ASR) is wider than the ESR. Hence, the diffusion of single species could act as a survival mechanism for species with initial densities below $w_2 = T$, but nearby ESR. Moreover, panel (d) of Fig. 4 shows that ESR does not cover the entire special domain, but the diffusion may give rise to survival everywhere.

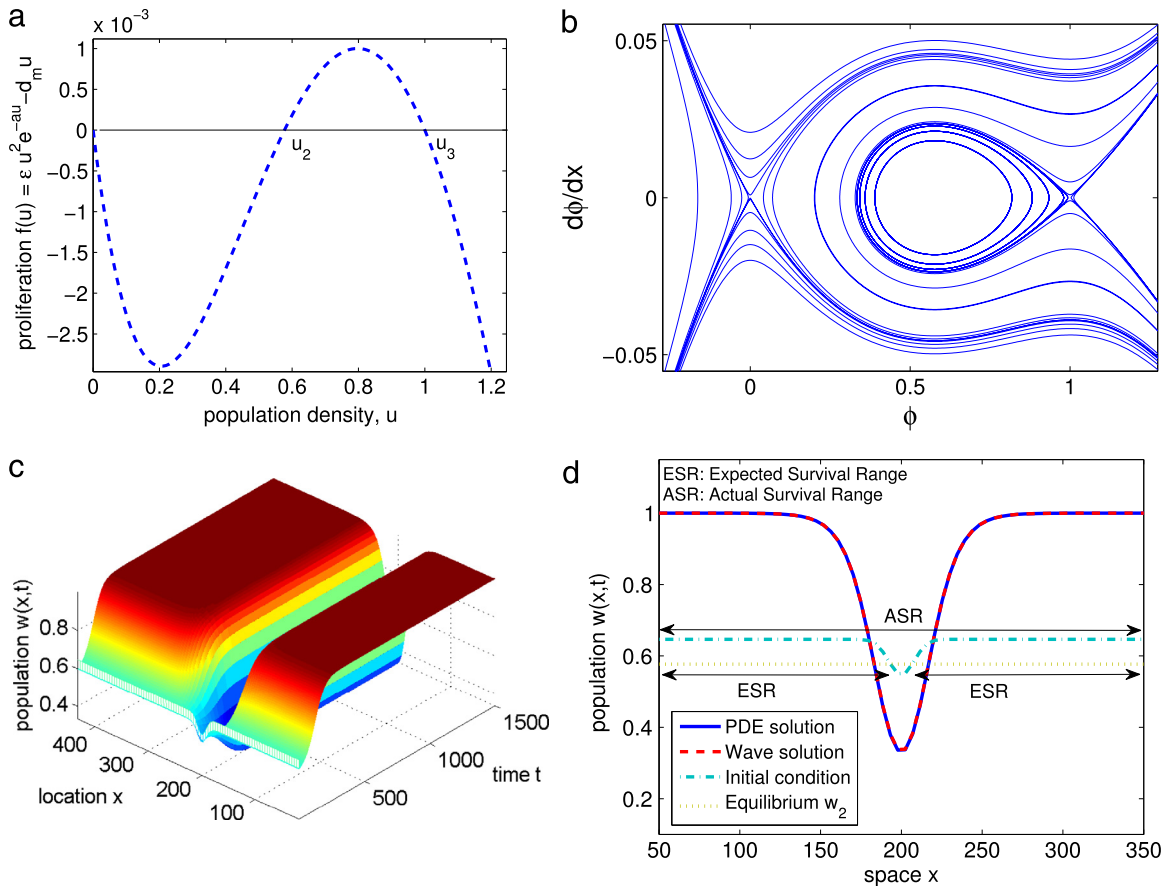


Fig. 4. The solution of the general model (4) may converge to the stationary inverted wave pulse. (a) Graph of the proliferation function $f(u) = \epsilon b(u) - d_m u$, with $F(1) < 0$ i.e., the area above $f(u)$, $u \in [0, u_2]$ is greater than the area under $f(u)$, $u \in [u_2, u_3]$. (b) Phase-plane of the system (9) representing a left-homoclinic orbit. (c and d) Convergence of the solution $w(x, t)$ of model (4) to the stationary inverted wave pulse $\phi(x)$ of the wave equation (13). See the supplementary file “coninvertpulse.gif” for the related animation (see Appendix A). In the absence of diffusion, the expected survival range corresponds to the regions with initial population densities above the threshold equilibrium $T = u_2$. Whereas the actual survival range corresponds to the entire special domain. The specific parameter values are given in Table 1.

4. Discussion

There have been widespread and extensive studies on delay diffusive models describing different biological situations. The population models based on Smith–Thieme and Britton’s approaches [22–24] have brought intensive activities to different areas of biology such as ecology, epidemiology and population biology. The local and global dynamics of these models are still of great interest and the possible outcomes of these models may bring significant insights in understanding the complicated nature of population growth and dispersal.

The primary focus of the present work was to investigate the existence and global stability of the stationary waves of both reduced and general models (7) and (4). As mentioned in Theorem 2 a stationary wave solution of the reduced model (7) is also a stationary wave solution of the general model (4). The numerical simulations suggest that the solution of the general model (4) may converge to the stationary wave solution satisfying Eqs. (8) and (13). The general model (4) may also admit stationary waves that are not those of the reduced model (7). Such stationary waves were not investigated in this paper. Formation of the stationary wave pulses and wavefront may reflect population establishment and colonization in certain regions of the wildlife habitats. The biological interpretations of conditions (H_1) – (H_4) and their subsequent results (i.e., Theorem 1 and Corollaries 1 and 2) are briefly discussed as follows. In the absence of population dispersal (i.e., diffusion), a single species population with strong Allee effect is expected to go extinct when the density falls below the threshold T . However, the present work shows that population dispersal may contribute to survival of species with initial densities less than T . For instance, Fig. 3(d) shows that a single species with initial densities below $T = 0.36$ but in the range $150 < x < 250$ may survive due to existence of a stable stationary wave pulse. Figs. 2(c) and 3(c) show that the actual survival regions may not necessarily match with the regions that have initial densities above $T = 0.45$ and $T = 0.36$, respectively. This is due to the fact that the shape of and amplitude of the stationary waves are not the same as the initial density curves defined by Eqs. (24) and (25), respectively. Therefore, the fate of the single species population can

be determined according to the shape (i.e., front, pulse or inverted pulse) of the globally stable stationary wave rather than a single threshold value T .

In conclusion, the present study was an effort to explore the existence and stability of the stationary waves of single species populations. Formation of the stationary waves in the spatial domain indicates that a constant threshold density does not necessarily determine the survival or extinction of single species with strong Allee effect.

Acknowledgment

This work was partially supported by the University of Missouri Research Board grant (ID: KZ016055).

Appendix A. Supplementary data

Supplementary material related to this article can be found online at <http://dx.doi.org/10.1016/j.cam.2015.11.021>.

References

- [1] M. Bani-Yaghoub, D.E. Amundsen, Dynamics of notch activity in a model of interacting signaling pathways, *Bull. Math. Biol.* 72 (4) (2010) 780–804.
- [2] N.F. Britton, *Reaction–Diffusion Equations and their Applications to Biology*, Academic Press, New York, 1986.
- [3] P. Grindrod, *The Theory and Applications of Reaction–Diffusion Equations–Patterns and Waves*, Oxford Univ. Press, New York, 1996.
- [4] J.H. Wu, *Theory and Applications of Partial Functional Differential Equations*, in: *Applied Math. Sci.*, vol. 119, Springer-Verlag, New York, 1996.
- [5] M. Bani-Yaghoub, D.E. Amundsen, Oscillatory traveling waves for a population diffusion model with two age classes and nonlocality induced by maturation delay, *J. Comput. Appl. Math.* 34 (1) (2014) 309–324.
- [6] J.W.-H. So, J. Wu, X. Zou, A reaction–diffusion model for a single species with age–structure. I Traveling wavefronts on unbounded domains, *Proc. R. Soc. Lond. Ser. A Math. Phys. Eng. Sci.* 457 (2001) 1841–1853.
- [7] R. Kapral, K. Showalter (Eds.), *Chemical Waves and Patterns*, Kluwer, Dordrecht, 1995.
- [8] A.I. Volpert, V.A. Volpert, V.A. Volpert, *Traveling Wave Solutions of Parabolic Systems*, in: *Translations of Mathematical Monographs*, vol. 140, American Mathematical Society, Providence, RI, 1994.
- [9] N. Akhmediev, A. Ankiewicz, *Solitons: Nonlinear Pulses and Beams*, Chapman and Hall, London, 1997.
- [10] L. Debnath, *Nonlinear Water Waves*, Academic Press, Boston, 1994.
- [11] F. Dias, C. Kharif, *Nonlinear gravity and capillary–gravity waves*, *Annu. Rev. Fluid Mech.* 31 (1999) 301–346.
- [12] R.S. Johnson, *A Modern Introduction to the Mathematical Theory of Water Waves*, Cambridge Univ. Press, Cambridge, 1997.
- [13] J. Smoller, *Shock Waves and Reaction–Diffusion Equations*, Springer, New York, 1994.
- [14] P.C. Fife, *Patterns formation in gradient systems*, in: B. Fiedler, G. Iooss, N. Kopell (Eds.), *Handbook of Dynamical Systems III: Towards Applications*, Elsevier, Amsterdam, 2000.
- [15] H.L. Smith, *Monotone Dynamical Systems: An Introduction to the Theory of Competitive and Cooperative Systems*, American Mathematical Society, 1995, ISBN: 10: 082180393X.
- [16] H. Smith, H. Thieme, Strongly order preserving semiflows generated by functional differential equations, *J. Differ. Equ.* 93 (1991) 332–363.
- [17] H.R. Thieme, *Mathematics in Population Biology*, Princeton University Press, Princeton, 2003.
- [18] J. Guckenheimer, P. Holmes, *Nonlinear Oscillations, Dynamical Systems, and Bifurcations of Vector Fields*, Springer-Verlag, New York, 1983.
- [19] D.W. Jordan, P. Smith, *Nonlinear Ordinary Differential Equations: An Introduction to Dynamical Systems*, Oxford University Press, 1999.
- [20] W.C. Allee, Animal aggregations, *Q. Rev. Biol.* 2 (1927) 367–398.
- [21] W.C. Allee, *Animal Aggregations: A Study in General Sociology*, Chicago Univ. Press, Chicago, 1933.
- [22] N.F. Britton, Aggregation and the competitive exclusion principle, *J. Theoret. Biol.* 136 (1) (1989) 57–66.
- [23] N.F. Britton, Spatial structures and periodic travelling waves in an integro-differential reaction–diffusion population model, *SIAM J. Appl. Math.* 50 (6) (1990) 1663–1688.
- [24] H. Smith, H. Thieme, Strongly order preserving semiflows generated by functional differential equations, *J. Differential Equations* 93 (1991) 332–363.
- [25] M. Bani-Yaghoub, G. Yao, Modeling and numerical simulations of single species dispersal in symmetrical domains, *Int. J. Appl. Math.* 27 (6) (2014) 525–547.
- [26] D. Liang, J. Wu, F. Zhang, Modelling population growth with delayed nonlocal reaction in 2-dimensions, *Math. Biosci. Eng.* 2 (1) (2005) 111–132.
- [27] P. Weng, D. Liang, J. Wu, Asymptotic patterns of a structured population diffusing in a two-dimensional strip, *Nonlinear Anal.* 69 (2008) 3931–3951.
- [28] M.C. Memory, Bifurcation and asymptotic behaviour of solutions of a delay-differential equation with diffusion, *SIAM J. Math. Anal.* 20 (1989) 533–546.
- [29] J.W.-H. So, J. Wu, Y. Yang, Numerical Hopf bifurcation analysis on the diffusive Nicholson's blowflies equation, *Appl. Math. Comput.* 111 (2000) 53–69.
- [30] J.W.-H. So, Y. Yang, Dirichlet problem for the diffusive Nicholson's blowflies equation, *J. Differential Equations* 150 (1998) 317–348.
- [31] D. Liang, J. Wu, Travelling waves and numerical approximations in a reaction advection diffusion equation with nonlocal delayed effects, *J. Nonlinear Sci.* 13 (2003) 289–310.
- [32] M. Bani-Yaghoub, G. Yao, M. Fujiwara, D.E. Amundsen, Understanding the interplay between density dependent birth function and maturation time delay using a reaction–diffusion population model, *Ecol. Complex.* 21 (2015) 14–26.
- [33] M. Bani-Yaghoub, Approximate traveling wave solution for a delayed nonlocal reaction–diffusion equation, *J. Appl. Math. Comput.* (2015) <http://dx.doi.org/10.1007/s12190-015-0958-7>.
- [34] R.W. Hamming, *Methods of Mathematics Applied to Calculus, Probability, and Statistics*, Dover ed., Dover Publications, 2004.